Naval Research Laboratory
Washington, DC 20375-5000

NRL Report 9168

Film Elastic Properties Determined by the Indentation Test—Theoretical Considerations

H. Y. YU

Geo-Centers Inc.
Fort Washington, MD 20744

S. C. SANDAY

Composites and Ceramics Branch
Materials Science and Technology Division

and

B. B. RATH

Materials Science and Component Technology Directorate

January 12, 1989

SECURITY CLASSIFICATION OF THIS PAGE

REPORT DOCUMENTATION PAGE

Form Approved
OMB No 0704-0188

1a REPORT SECURITY CLASSIFICATION UNCLASSIFIED	1b RESTRICTIVE MARKINGS
2a SECURITY CLASSIFICATION AUTHORITY	3 DISTRIBUTION/AVAILABILITY OF REPORT Approved for public release; distribution unlimited
2b DECLASSIFICATION/DOWNGRADING SCHEDULE	
4 PERFORMING ORGANIZATION REPORT NUMBER(S) NRL Report 9168	5 MONITORING ORGANIZATION REPORT NUMBER(S)
6a NAME OF PERFORMING ORGANIZATION Naval Research Laboratory 6b OFFICE SYMBOL (If applicable) Code 6370	7a NAME OF MONITORING ORGANIZATION
6c ADDRESS (City, State, and ZIP Code) Washington, DC 20375-5000	7b ADDRESS (City, State, and ZIP Code)
8a NAME OF FUNDING/SPONSORING ORGANIZATION Office of Naval Research 8b OFFICE SYMBOL (If applicable)	9 PROCUREMENT INSTRUMENT IDENTIFICATION NUMBER
8c ADDRESS (City, State, and ZIP Code) Arlington, VA 22217	10 SOURCE OF FUNDING NUMBERS PROGRAM ELEMENT NO: 61153N; PROJECT NO: RR0220441; TASK NO:; WORK UNIT ACCESSION NO: DN280-063

11 TITLE (Include Security Classification)

Film Elastic Properties Determined by the Indentation Test—Theoretical Considerations

12 PERSONAL AUTHOR(S)
Yu, H. Y., Sanday, S. C., and Rath, B. B.

13a TYPE OF REPORT	13b TIME COVERED	14 DATE OF REPORT (Year, Month, Day)	15 PAGE COUNT
Interim	FROM _____ TO _____	1989 January 12	34

16 SUPPLEMENTARY NOTATION

17 COSATI CODES			18 SUBJECT TERMS (Continue on reverse if necessary and identify by block number)
FIELD	GROUP	SUB-GROUP	Indentation; Layered material; Elastic solution; Elastic constants

19 ABSTRACT (Continue on reverse if necessary and identify by block number)

The elastic solutions of axisymmetric mixed boundary value problems are considered. An elastic layer is assumed to be either in smooth contact or perfectly bonded to a semi-infinite elastic half-space. The elastic field caused by the indentation of the elastic layer by a rigid indenter is solved for spherical, conical, and flat-ended-cylindrical indenters. The results are obtained by solving a Fredholm integral equation of the second kind with a continuous symmetrical kernel that depends on the bonding conditions. Numerical results are given for several combinations of film and substrate elastic moduli and film thicknesses. These results provide a guideline for selecting appropriate film thickness and substrates to determine the elastic constants of thin films.

20 DISTRIBUTION/AVAILABILITY OF ABSTRACT ☒ UNCLASSIFIED/UNLIMITED ☐ SAME AS RPT ☐ DTIC USERS	21 ABSTRACT SECURITY CLASSIFICATION UNCLASSIFIED
22a NAME OF RESPONSIBLE INDIVIDUAL S. C. Sanday	22b TELEPHONE (Include Area Code) (202) 767-2264 22c OFFICE SYMBOL Code 6370

DD Form 1473, JUN 86 *Previous editions are obsolete* SECURITY CLASSIFICATION OF THIS PAGE

CONTENTS

FILM ELASTIC PROPERTIES DETERMINED BY THE INDENTATION TEST—THEORETICAL CONSIDERATIONS

INTRODUCTION

Intense interest in thin-film technology has been spurred by the growing importance of microelectronics, metal matrix composites, ceramic matrix composites, high transition temperature superconducting films, and compositionally modulated materials. Correspondingly, the determination of film properties has become of greater importance. The need for techniques to study the mechanical properties of thin films, which are usually defined as coatings of thickness of up to a few micrometers, has recently rekindled an interest in microhardness and submicroindentation devices. The continuous indentation test, also known as the impression test, measures the elastic constants of bulk materials [1-3]. In these tests, the displacement and the load of the indenter, which is pressed onto a specimen at a predetermined speed, is recorded. The slope of the unloading curves in the load vs depth plot determines the elastic modulus of the specimen. Recently, a high-resolution nanoindenter was used to determine the Young's modulus of thin films [4] from the linear unloading portion of the indentation load vs depth curves. It was also shown that, as the indentation depth d approaches the dimension of the film thickness h, the influence of the substrate can be detected because of the changing contributions of the film and the substrate to the measured elastic constant. For small indentation depth relative to the film thickness, the data approach that expected for bulk film material since the indenter interrogates the film near its surface only. For deep indentations, the data approach that expected for bulk substrate material.

The indentation problem is a mixed boundary value problem, more commonly known as Boussinesq's problem. Harding and Sneddon [5], Sneddon [6], and Miki [7] have considered this problem when a semi-infinite space is indented by a cone, a sphere, and a flat-ended cylindrical punch. The flat-ended cylindrical punch problem for an elastic layer resting frictionlessly on a rigid foundation has been considered by Lebedev and Ufliand [8]. The rigid substrate supporting the elastic layer is, of course, a mathematical artifice that simplifies the analysis. Some investigators considered the indentation of an elastic layer perfectly bonded to an elastic half-space made up of different materials. Wu and Chiu [9] considered the plane strain problem and reduced the mixed boundary value problem to a single Fredholm integral equation of the second kind. Dhaliwal [10] was able to reduce the axisymmetric problem of a flat-ended cylindrical punch on a layered elastic medium to a Fredholm integral equation, which he solved approximately to estimate the safety of foundations supporting cylindrical columns. Subsequently Dhaliwal and Rau [11] extended the analysis of Dhaliwal to punches of arbitrary profile but did not present any numerical results.

A second approach to the solution of mixed boundary value problems is to replace the exact boundary condition by an approximate one and solve the new elasticity problem. Chen and Engel [12] used this approach to study the impact and contact stresses caused by flat-ended cylindrical and parabolic punches on a composite medium consisting of one or two elastic layers perfectly bonded to each other and to an elastic homogeneous half-space.

Manuscript approved August 16, 1988.

The punch problem (for any shape punch) for an elastic layer resting frictionlessly on an elastic substrate (half-space) has not been considered. The punch problems for conical or spherical punches for a layer perfectly bonded to an elastic substrate have not been considered either. The need for the solution of these problems for determining the elastic properties of thin films by the indentation test is obvious. The contact between the thin film and the substrate is neither frictionless nor perfectly bonded. The solutions and numerical values for both ideal cases should be obtained to set guidelines for the indentation test, i.e., to determine what the proper substrate is and what the required film thickness is so that the film's elastic constants may be measured within a predetermined degree of accuracy. These are goals of this investigation.

FORMULATION OF THE PROBLEM

Consider an infinite layer of thickness h with elastic constants μ_1, ν_1, overlaying a half-space substrate with elastic constants μ_2, ν_2, and a rigid axisymmetric indenter (punch) with a flat, conical, or hemispherical end (Figs. 1 to 3, respectively) and axis normal to the layer surface, pressing frictionlessly on the layer. Choose cylindrical coordinate axes (r, θ, z) such that z is parallel to the generatrix of the indenter, r is perpendicular to z, θ is the angular distance between a reference line and r, and the origin of coordinates is located at the first point of contact between the indenter and the layer (center of first contact area for the flat-ended indenter).

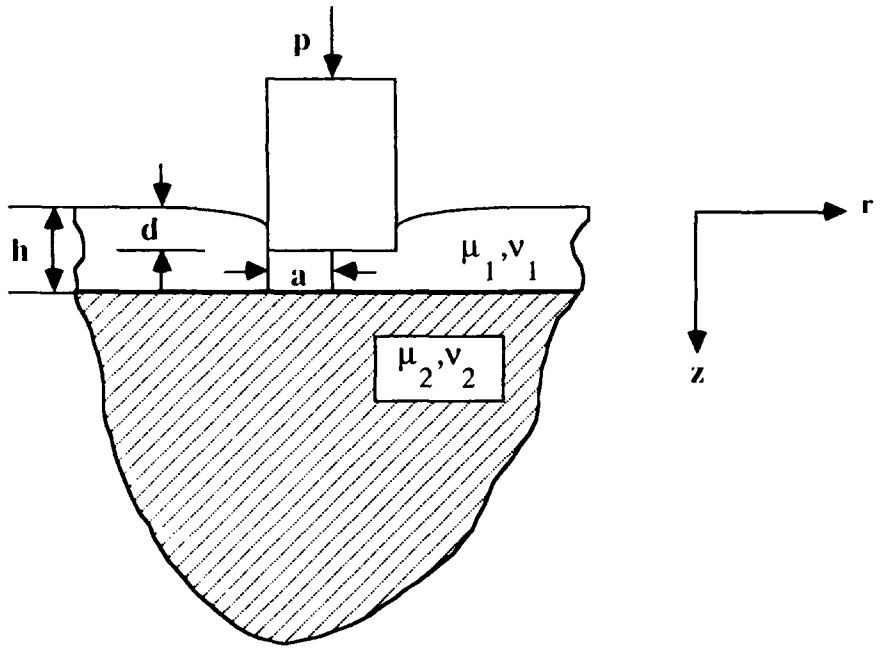

Fig. 1 — A composite medium consisting of an elastic layer either perfectly bonded to or smoothly overlaying an elastic semi-infinite substrate indented by a rigid flat-ended cylindrical indenter

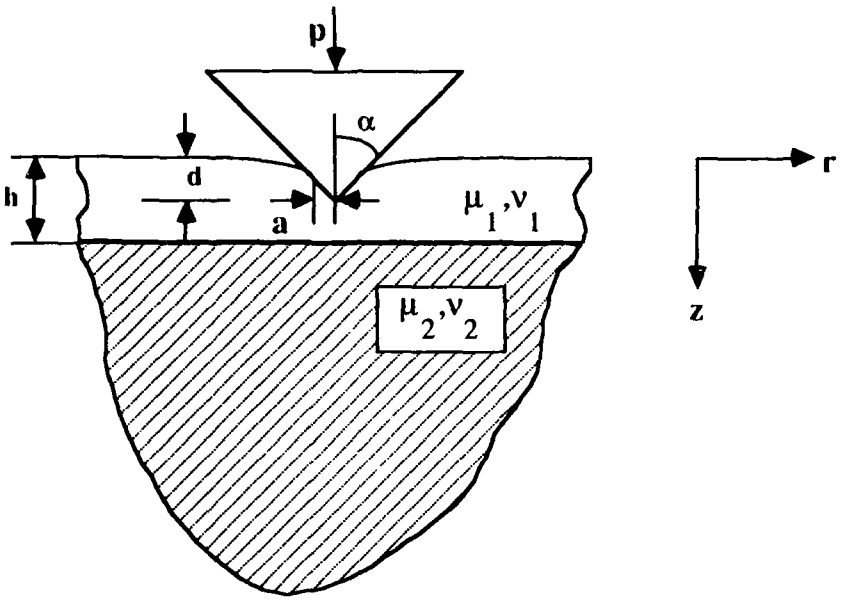

Fig. 2 — A composite medium consisting of an elastic layer either perfectly bonded to or smoothly overlaying an elastic semi-infinite substrate indented by a rigid conical indenter

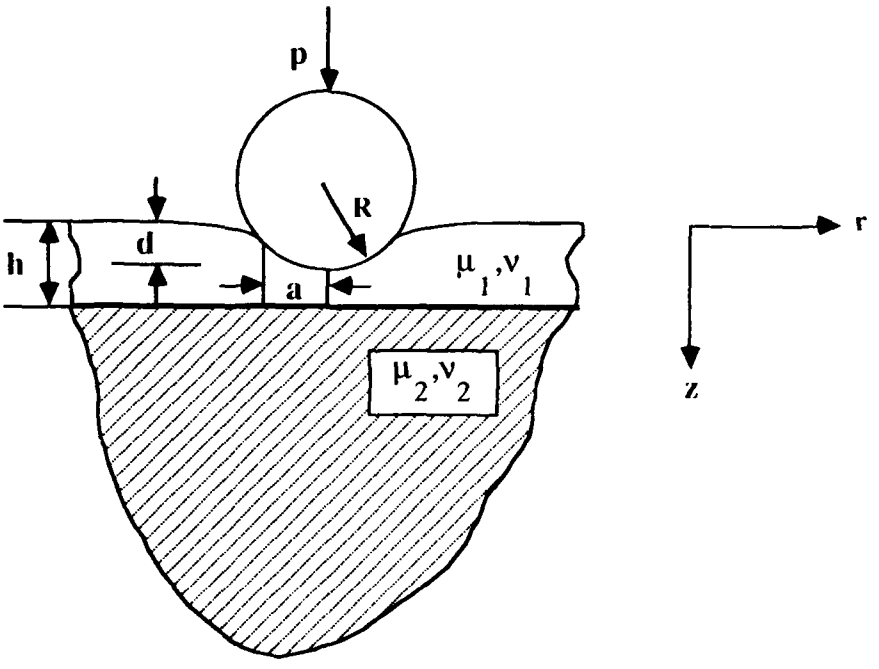

Fig. 3 — A composite medium consisting of an elastic layer either perfectly bonded to or smoothly overlaying an elastic semi-infinite substrate indented by a rigid spherical indenter

The Papkovich-Neuber functions may then be used to formulate the problem. Thus, in terms of a pair of harmonic functions $\varphi_j\ (r, z)$ and $\Psi_j\ (r, z)$ $(j = 1, 2)$, the displacement and stress components of interest may be written as

$$\begin{aligned} 2\mu_j u_{rj} &= -\varphi_{j,r} - z\Psi_{j,r}, \\ 2\mu_j u_{zj} &= k_j\Psi_j - \varphi_{j,z} - z\Psi_{j,z}, \\ \sigma_{zj} &= 2(1-\nu_j)\Psi_{j,z} - \varphi_{j,zz} - z\Psi_{j,zz}, \\ \tau_{rzi} &= (1-2\nu_j)\Psi_{j,r} - \varphi_{j,rz} - z\Psi_{j,rz}, \text{ and} \\ j &= 1, 2,\ k_j = 3 - 4\nu_j, \end{aligned} \tag{1}$$

where the letter subscripts following a comma denote differentiation with respect to the indicated cylindrical coordinates, e.g., $\varphi_{j,rz} = \partial^2\varphi_j/\partial r\,\partial z$.

The harmonic functions $\varphi_j(r, z)$, $\Psi_j(r, z)$ may be expressed in terms of a new set of unknown functions $A_i(\lambda)$, $(i = 1, 2, \ldots, 6)$ as the following Hankel integrals

$$\begin{aligned} \Psi_1(r, z) &= \int_0^\infty (A_1 \operatorname{ch}\lambda z + A_2 \operatorname{sh}\lambda z)\frac{J_0(\lambda r)}{\operatorname{sh}\lambda h}\,d\lambda, \\ \varphi_1(r, z) &= \int_0^\infty (A_3 \operatorname{sh}\lambda z + A_4 \operatorname{ch}\lambda z)\,\frac{J_0(\lambda r)}{\lambda \operatorname{sh}\lambda h}\,d\lambda, \\ \Psi_2(r, z) &= \int_0^\infty A_5 e^{-\lambda(z-h)}J_0(\lambda r)\,d\lambda, \\ \varphi_2(r, z) &= \int_0^\infty A_6 e^{-\lambda(z-h)}\,\frac{J_0(\lambda r)}{\lambda}\,d\lambda, \end{aligned} \tag{2}$$

where ch λz and sh λz are hyperbolic cosine of λz and hyperbolic sine of λz respectively and $J_0(\lambda r)$ is the Bessel function of the first kind of order 0. It may be readily be seen that Eqs. (2) satisfy the boundary conditions that the stresses and their derivatives in both media vanish for $r \geq 0$, $z \to \infty$, and for $z > 0$, $r \to \infty$.

Regardless of type of contact between layer and substrate the displacement and traction boundary conditions of the surface may be expressed as

$$u_{z1}(r, 0) = d - \delta(r/a) \qquad (0 \leq r \leq d), \tag{3.1}$$

$$\sigma_{z1}(r,0) = 0 \qquad (a < r < \infty), \text{ and} \tag{3.2}$$

$$\tau_{rz1}(r,0) = 0 \qquad (0 \leq r < \infty), \tag{3.3}$$

where d is the depth of penetration of the indenter, a is the radius of the circle of contact, and the function $\delta(r/a)$ is prescribed by the fact that, in reference to the tip of the indenter as origin, the punch has equation $z = \delta(r/a)$ so that $\delta(0) = 0$. The function $\delta(r/a)$ for conical, hemispherical, and flat-ended cylindrical indenters on the half-space have been given by Sneddon [6].

With the functions $\varphi_j(r, z)$ and $\Psi_j(r, z)$ $(j = 1, 2)$ as shown in Eq. (2), the boundary conditions Eq. (3.1) to (3.3) may be expressed by using Eq. (1) as follows:

$$\int_0^\infty \frac{A_1(\lambda)}{\operatorname{sh} \lambda h} J_0(\lambda r)\, d\lambda = \frac{\mu_1}{1 - \nu_1} [d - \delta(r/a)] \qquad (0 \le r \le a), \tag{4.1}$$

$$\int_0^\infty \frac{A_4(\lambda) - 2(1 - \nu_1)A_2(\lambda)}{\operatorname{sh} \lambda h} \lambda J_0(\lambda r)\, d\lambda = 0 \qquad (a < r < \infty), \tag{4.2}$$

and

$$A_3(\lambda) = (1 - 2\nu_1)A_1(\lambda) \qquad (0 < r < \infty). \tag{4.3}$$

Defining

$$M(\lambda) = \frac{A_1(\lambda)}{\operatorname{sh} w}, \; 1 - g(\lambda) = \frac{A_1(\lambda)}{A_4(\lambda) - 2(1 - \nu_1)A_2(\lambda)}, \tag{5}$$

where $w = \lambda h$, and the conditions Eqs. (4.1) and (4.2) lead to a system of two integral equations for $M(\lambda)$:

$$\int_0^\infty M(\lambda) J_0(\lambda r)\, d\lambda = f(r) \qquad (0 \le r \le a), \tag{6.1}$$

and

$$\int_0^\infty \frac{\lambda M(\lambda)}{1 - g(\lambda)} J_0(\lambda r)\, d\lambda = 0 \qquad (a < r < \infty), \tag{6.2}$$

where

$$f(r) = \frac{\mu_1}{1 - \nu_1} [d - \delta(r/a)]. \tag{7}$$

The function $g(\lambda)$ can be obtained, as shown in detail in the Appendix A, by expressing the unknown functions $A_i(\lambda)$ $(i = 1, 2, \ldots, 6)$ in terms of $A_1(\lambda)$ for different boundary conditions between the layer and the semi-infinite half-space. This is, for the case of perfect bonding, continuity of components of displacements and tractions at $z = h$ requires that

$$\begin{aligned} u_{r1}(r, h) &= u_{r2}(r, h), \\ u_{z1}(r, h) &= u_{z2}(r, h), \\ \sigma_{z1}(r, h) &= \sigma_{z2}(r, h), \text{ and} \\ \tau_{rz1}(r, h) &= \tau_{rz2}(r, h), \end{aligned} \tag{8}$$

for $0 \leq r \leq \infty$, while for the case when the two surfaces are in smooth contact (frictionless), continuity of normal components of displacement and tractions and the conditions of vanishing shear stress components at the interface may be expressed by

$$\begin{aligned} u_{z1}(r, h) &= u_{z2}(r, h), \\ \sigma_{z1}(r, h) &= \sigma_{z2}(r, h), \text{ and} \\ \tau_{rz1}(r, h) &= \tau_{rz2}(r, h) = 0, \end{aligned} \tag{9}$$

for $0 \leq r < \infty$.

The solution of Eq. (6) is sought in the form [9]

$$M(\lambda) = [1 - g(\lambda)] \int_0^a \phi(t) \cos \lambda t \, dt, \tag{10}$$

where $\phi(t)$ is the solution of the following Fredholm integral equation of the second kind with a continuous symmetrical kernel:

$$\phi(t) - \frac{1}{\pi} \int_0^a [G(s + t) + G(s - t)] \phi(s) \, ds = F(t) \qquad (0 \leq t \leq a), \tag{11}$$

where

$$G(x) = \int_0^\infty g(\lambda) \cos \lambda x \, d\lambda, \tag{12}$$

$$F(t) = \frac{2}{\pi} [f(0) + t \int_0^{\frac{\pi}{2}} f'(t \sin \theta) \, d\theta], \tag{13}$$

and

$$f'(x) = \frac{d}{dx} f(x).$$

After determining $F(t)$, the unknown function $\phi(t)$ can be solved by using Eq. (11). Then by using Eq. (10) and the solutions of the simultaneous equations of $A_i(\lambda)$, Eqs. (1) and (2) give a complete solution to the contact problem under consideration. For instance, by using Eq. (2) and the known formula

$$\begin{aligned} \int_0^\infty J_0(\lambda r) \sin \lambda t \, d\lambda &= 0 \qquad (0 \leq t < r), \\ &= (t^2 - r^2)^{-1/2} \qquad (t > r), \end{aligned} \tag{14}$$

it is easy to obtain the equation for the distribution of the normal stresses under the punch

$$\sigma_{z1}(r, 0) = \int_r^a \frac{\phi'(t)}{(t^2 - r^2)^{1/2}} \, dt - \frac{\phi(a)}{(a^2 - r^2)^{1/2}} \qquad (r < a). \tag{15}$$

Substituting Eq. (7) into Eq. (13) we have

$$F(t) = \frac{2\mu_1 d}{\pi(1 - \nu_1)} F_0(\tau), \tag{16}$$

where

$$F_0(\tau) = 1 - \frac{\delta(0)}{d} - \frac{\tau}{d} \int_0^{\frac{\pi}{2}} \delta'(\tau \sin \theta)\, d\theta, \tag{17}$$

and $\tau = t/a$. Introducing the dimensionless quantities

$$\frac{s}{a} = y \quad \text{and} \quad \phi(t) = \frac{2\mu_1 d}{\pi(1 - \nu_1)} H(\tau), \tag{18}$$

Eq. (11) then assumes the form

$$H(\tau) - \frac{1}{\pi} \int_0^1 [K(y + \tau) + K(y - \tau)]\, H(y)\, dy = F_0(\tau) \qquad (0 \leq \tau \leq 1), \tag{19}$$

where

$$K(u) = \frac{a}{h} \int_0^\infty g(w) \cos\left[\frac{auw}{h}\right] dw. \tag{20}$$

The magnitude of the applied load p can be obtained by integrating the pressure of the indenter on the layer over the area of contact, i.e., integrating Eq. (15) over the area of the circle of radius a. Thus,

$$p = \frac{4\mu_1 ad}{1 - \nu_1} \int_0^1 H(\tau)\, d\tau, \tag{21}$$

where $H(\tau)$ is known after $F_0(\tau)$ in Eq. (19) is determined.

The function $F_0(\tau)$ can be obtained from Eqs. (9), (13), (16), and (17) for an indenter of arbitrary axisymmetric profile. Intuitively, the contact pressure for the top surface of the layered half-space and that for the homogeneous half-space are similar in many respects if the indenter profile remains the same in both cases. For example, if the indenter has a sharp corner, the stress will be singular there. If the idenier profile is smooth, then the normal stress σ_{z1} must, on physical grounds, remain finite around the circle $r = a$ ($\tau = 1$). This continuity of normal stresses gives an additional equation

$$\phi(a) = H(1) = 0, \tag{22}$$

which is a consequence of Eqs. (15) and (18). Therefore, in the case of indenters with smooth profile, such as conical or hemispherical, Eqs. (19) and (22) have to be solved first to find the relationships between the penetration depth d and the radius of contact area a. For convenience, let us define a dimensionless parameter γ, which is a function of h, μ_1, ν_1, μ_2, ν_2, and the indenter profile,

$$\gamma = \frac{a}{a_H}, \tag{23}$$

where a_H is the radius of the contact area for a homogeneous half-space with elastic constants μ_1 and ν_1. The relationships between a_H and d for different indenters are [5];

$$a_H = a, \tag{24}$$

for a flat-ended cylindrical indenter of radius a (note that this equation is independent of d);

$$a_H = \frac{2}{\pi} d \tan \alpha, \tag{25}$$

for a conical indenter with included angle 2α; and

$$a_H = 2d \left(\ln \frac{1 + \rho}{1 - \rho} \right)^{-1} \qquad (\rho = a_H/R),$$

$$= (Rd)^{1/2} \qquad (a_H << R), \tag{26}$$

for a hemispherical tip indenter of radius R.

Since when using the indentation test to determine elastic constants, such as Young's modulus, shear modulus, or Poisson ratio, each constant is not measured directly but in any combinations of pairs, it is convenient to define a new elastic constant, say

$$\zeta = \frac{4\mu}{1 - \nu}, \tag{27}$$

which may be called the impression elastic modulus, or the impression modulus for short. Now the relationship between p and z for each type of indenter may be obtained as follows.

Flat-ended Cylindrical Indenter

For the flat-ended cylindrical indenter of radius a (Fig. 1), the boundary condition Eq. (3.1) is

$$u_{z1}(r, 0) = d \qquad (0 \leq r \leq d),$$

which gives

$$\delta(r/a) = 0, f(r) = \frac{1}{4} \zeta_1 d \qquad (0 \leq r \leq a),$$

and

$$F_0(\tau) = 1 \qquad (0 \leq \tau \leq 1), \tag{28}$$

where ζ_1 is the impression modulus for the homogeneous half-space with elastic constants μ_1 and ν_1. According to Eq. (21), the relationship between the p and the d can be written as

$$P = \zeta_1 ad \int_0^1 H(\tau)\, d\tau, \tag{29}$$

and

$$p_i = \zeta_i ad \qquad (i = 1, 2), \tag{30}$$

where $i = 1$ when $h \to \infty$ and $i = 2$ and $h \to 0$.

Conical Indenter

For normal penetration by a rigid cone of included angle 2α (Fig. 2), the boundary condition, Eq. (3.1), gives

$$\delta(r/a) = r \cot \alpha \qquad (0 \le r \le a), \tag{31}$$

then Eqs. (7) and (13) become

$$f(r) = \frac{1}{4}\, \zeta_1 d \left[1 - \frac{2\gamma_c}{\pi a} r\right] \qquad (0 \le r \le a).$$

and

$$F_0(\tau) = 1 - \gamma_c \tau \qquad (0 \le \tau \le 1), \tag{32}$$

where $\gamma_c = a/a_H$. The relationships between p, d, and a are

$$\begin{aligned} p &= \frac{2}{\pi}\, \gamma_c \zeta_1 d^2 \tan \alpha \int_0^1 H(\tau)\, d\tau, \\ &= \frac{\pi}{2}\, \gamma_c \zeta_1 a_H^2 \cot \alpha \int_0^1 H(\tau)\, d\tau, \end{aligned} \tag{33}$$

and

$$p_i = \zeta_i d^2 \tan \alpha \qquad (i = 1, 2). \tag{34}$$

Spherical Indenter

For normal penetration by a rigid spherical indenter of radius R (Fig. 3), the same as before, the strained surface of the elastic layer conforms to the sphere between the first point of contact and the section of radius a. From the geometry of Fig. 3 we find that

$$\delta(r/a) = R \left[1 - \left(1 - \frac{r^2}{R^2}\right)^{1/2}\right] \qquad (0 \le r \le a). \tag{35}$$

which gives

$$f(r) = \frac{1}{4}\, \zeta_1 d \left[1 - \frac{2}{\gamma_s^2 \rho} \frac{1 - \left(1 - \frac{r^2}{R^2}\right)^{1/2}}{\ln(1 + \rho) - \ln(1 - \rho)}\right] \qquad (0 \le r \le a), \tag{36}$$

and

$$F_0(\tau) = 1 - \frac{\tau}{\gamma_s^2} \frac{\ln(1+\rho\tau) - \ln(1-\rho\tau)}{\ln(1+\rho) - \ln(1-\rho)} \qquad (0 \le \tau \le 1), \tag{37}$$

where $\gamma_s = a/a_H$ and $\rho = a/R$. If the indentation is small ($a << R$ or $\rho << 1$), then approximately

$$a = \gamma_s (Rd)^{1/2} \qquad (a << R), \tag{38}$$

and

$$F_0(\tau) = 1 - \gamma_s^2 \tau^2 \qquad (0 \le \tau \le 1,\ \rho << 1), \tag{39}$$

and from Eqs. (38) and (21)

$$\begin{aligned} p &= \gamma_s \zeta_1 R^{1/2} d^{3/2} \int_0^1 H(\tau) d\tau, \\ &= \gamma_s \zeta_1 R^{-1} a_H^3 \int_0^1 H(\tau)\, d\tau, \end{aligned} \tag{40}$$

and

$$p_i = \frac{2}{3} \zeta_i R^{1/2} d^{3/2} \qquad (i = 1, 2). \tag{41}$$

The formulation of the problem is now complete for each of the three types of indenter considered. Numerical results for some cases of interest are presented and discussed in the following section.

NUMERICAL RESULTS

The mixed boundary value problem is represented by the Fredholm integral equation of the second kind as shown in Eq. (19). For a given function $k(u)$ (Eq. (20)) and $F_0(\tau)$ (Eqs. (28), (31), or (35) depending on the shape of the indenter), the function $H(\tau)$ is solved numerically in the form of a Chebyshev series of N terms ($N \ge 5$) [13]. The load on the indenter is then obtained by integration as indicated in Eq. (21). The calculations of the load and the function $K(u)$ for the given function $g(\lambda)$ (see Appendix A, Eqs. (A2) and (A10)) are also carried out numerically by using a Cray supercomputer.

For the conical and the spherical indenters, Eq. (19) is first solved by setting the parameter γ equal to 1 and then iterating until a proper value for γ is obtained such that $H(1) = 0$. Then the correct γ values are used to solve the function $H(\tau)$ and the load p.

The papers of Lebedev and Ufliand [8], Dhaliwal [9], and Chen and Engel [12] contain some numerical results and thus provide an excellent opportunity for comparison with the results obtained here. The kernel $K(u)$, as defined by Eq. (20), is computed first for both an elastic layer in smooth contact with a rigid substrate and an elastic layer perfectly bonded to an elastic substrate. The results obtained are the same as those in Refs. 8 and 9 (Tables B1 and B2 in Appendix B). The computer program used to solve the Fredholm integral equation (Eq. 19) was further checked by computing $H(\tau)$ values for a flat-ended cylindrical indenter pressing on an elastic layer in smooth contact with a rigid substrate and comparing the results with those given by Lebedev and Ufliand [8]. The excellent agreement (Table B3) provided confidence in the correctness of the present analysis.

When the layer and the substrate are perfectly bonded and the indenter is a flat-ended cylinder, the $H(\tau)$ values calculated by using the same set of $K(u)$ values (Table B2) show substantial disagreement between our results and Dhaliwal's published results (Table B4), as noted, for example, for the case when $h/a = 0.25$ and $\mu_1/\mu_2 = 0$ where values for $H(\tau)$ differ by approximately an order of magnitude. However, the results of Chen and Engel [12] for the spherical indenter when $a << R$ were reproduced (Table B5). The details of these comparisons are given in Appendix B.

In the present calculation, the number of terms N in the Chebyshev series that approximate the solution $H(\tau)$ is taken to be 5 when $h/a > 0.5$. For values of h/a smaller than 0.5, the number of terms should be increased to get accurate values for $H(\tau)$. For example, in our calculation, N was chosen to be 25 when $h/a = 0.1$.

Figures 4 to 7 give the relationships between the parameter γ (Eq. 23) and the layer thickness h for different indenter shapes, layer and substrate elastic properties, and bonding conditions. The parameter γ is the radius of contact a normalized with respect to the Hertz contact radius a_H for a homogeneous half-space of shear modulus μ_1 and Poisson ratio ν_1. For conical and spherical indenters with smooth contact between layer and substrate, the results for $\eta = 0$, 0.2, 1,2, and 10 (where $\eta = (1 - \nu_2)\mu_1/(1 - \nu_1)\mu_2$) are plotted in Figs. 4 and 5, respectively. Figures 6 and 7 show the relationship between γ and h/a for a layer perfectly bonded to the substrate when $\beta = 0$, 0.2, 1, 2, and 10 (where $\beta = \mu_1/\mu_2$), and $\nu_1 = \nu_2 = 0.3$ for the conical and spherical indenters, respectively. These results show that $\gamma > 1$ when the substrate is stiffer than the layer ($\eta > 1$ or $\beta > 1$), and $\gamma < 1$ when the layer is stiffer than the substrate ($\eta < 1$ or $\beta < 1$). For a given depth of penetration, the radius of contact between the indenter and the composite medium increases with increasing stiffness of substrate materials. For a layer/substrate stiffness ratio (η or β) smaller than 1, the radius of contact increases from the value a_H to a certain maximum value and then decreases asymptotically back to the value a_H as the layer thickness increases from 0 to ∞. The layer thickness at which the maximum radius of contact occurs is always less than the radius of contact itself, i.e., $h/a < 1$. On the other hand, when the substrate is less stiff than the layer, the radius of contact decreases from its homogeneous half-space value a_H to a minimum value and then increases toward a_H asymptotically as the layer thickness h increases from 0 to ∞. The minimum value occurs in the range where $1 < h/a < 2$. Note that when the layer and the substrate are identical and there is no friction force at the interface, the radius of contact is not always the same as the homogeneous half-space, but it increases first, then decreases to a minimum value and increases again toward the homogeneous value a_H.

For the purpose of setting up a guideline for choosing the appropriate layer thickness and substrate properties to determine the elastic constants of thin films by the indentation test, it is convenient to define a nondimensional quantity p/p_1, which is the radio between p, the load needed to penetrate to a depth d into the composite (layered half-space) and p_1 the load needed to penetrate the same depth d into the homogeneous half-space consisting of the top layer material. This ratio p/p_1 is then plotted against h/a. For different shapes of indenter p/p_1 are given as follows:

$$\frac{p}{p_1} = \int_0^1 H(\tau)\, d\tau \qquad \text{(cylindrical indenter)},$$

$$\frac{p}{p_1} = 2\gamma_c \int_0^1 H(\tau)\, d\tau \qquad \text{(conical indenter)}, \tag{42}$$

and

$$\frac{p}{p_1} = \frac{3}{2}\gamma_s \int_0^1 H(\tau) d\tau \qquad \text{(spherical indenter)}.$$

Figures 8 through 13 show the p/p_1 vs h/a curves for the smooth contact condition (η = 0, 0.2, 0.5, 1, 2, and 10) and for perfectly bonded condition (β = 0, 0.2, 0.5, 1, 2, and 10, $\nu_1 = \nu_2 = 0.3$) for the flat-ended cylindrical indenter, the conical indenter, and the spherical indenter, respectively. When the layer is perfectly bonded to, and softer than the substrate, the load p on the composite decreases more or less exponentially from p_2 (the load for the homogeneous half-space with elastic constants μ_2 and ν_2) to p_1 (the load for the homogeneous half-space with elastic constants μ_1 and ν_1) as the thickness of the layer increases from 0 to ∞. On the other hand, when the layer is stiffer than the substrate, p increases asymptotically from p_2 to p_1. When the layer is in smooth contact with and stiffer than the substrate, p decreases from p_2 to a minimum value, then increases toward p_1 as the layer thickness varies from 0 to ∞. When the layer is softer than the substrate, p does not decrease asymptotically from p_2 to p_1; for μ_2/μ_1 less than certain value (for example 0.63 for the flat-ended cylindrical indenter as shown in Fig. 14), the p values decrease from p_2 to a minimum value less than p_1, then increase and approach p_1 as the thickness increases.

When the indenter is a flat-ended cylinder of radius a, the radius of the contact area is always equal to a regardless of the composite medium material and layer thickness. This means the parameter γ is always equal to 1. When the indenter is conical or spherical, the radius of the contact area is no longer a constant, but is a function of the penetration depth d, the layer thickness h, the elastic constants of the layer and the substrate, and the shape of the indenter. Therefore, the scale of the absissa h/a, in Figs. 10 to 13, are not the same for all the curves. To compare the results for different conditions, it is necessary to express h in units of the constant value a_H instead of the variable a. Figures 15 to 18 show the p/p_1 vs h/a_H curves that are converted from Figs. 9, 10, 12, and 13 by using the corresponding γ values from Figs. 4 to 7, respectively.

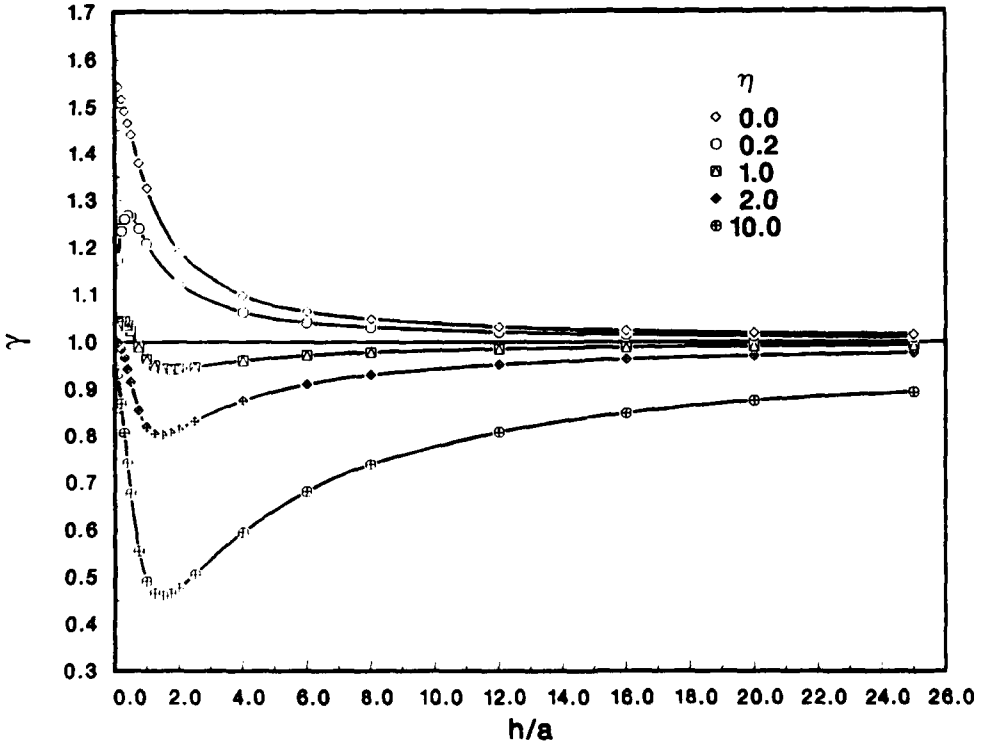

Fig. 4 — Variation of the normalized radius of the contact area between the conical indenter and the smooth contact composite medium γ, with layer thickness h/a, as a function of layer/substrate stiffness ratio η

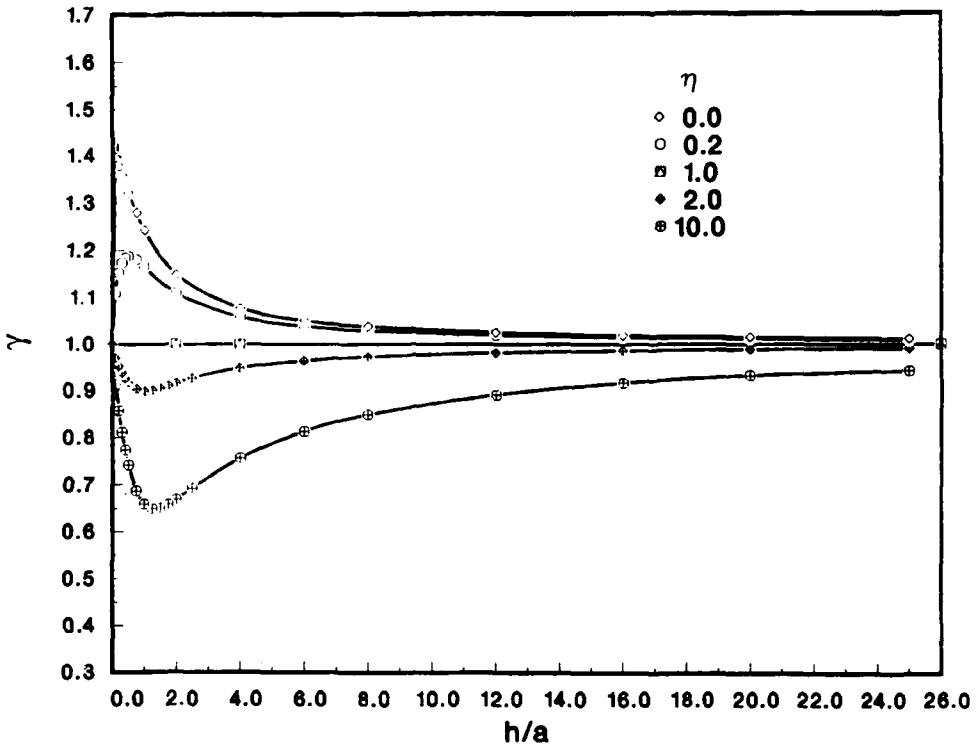

Fig. 5 — Variation of the normalized radius of the contact area between the spherical indenter and the smooth contact composite medium γ, with layer thickness h/a, as a function of layer/substrate stiffness ratio η

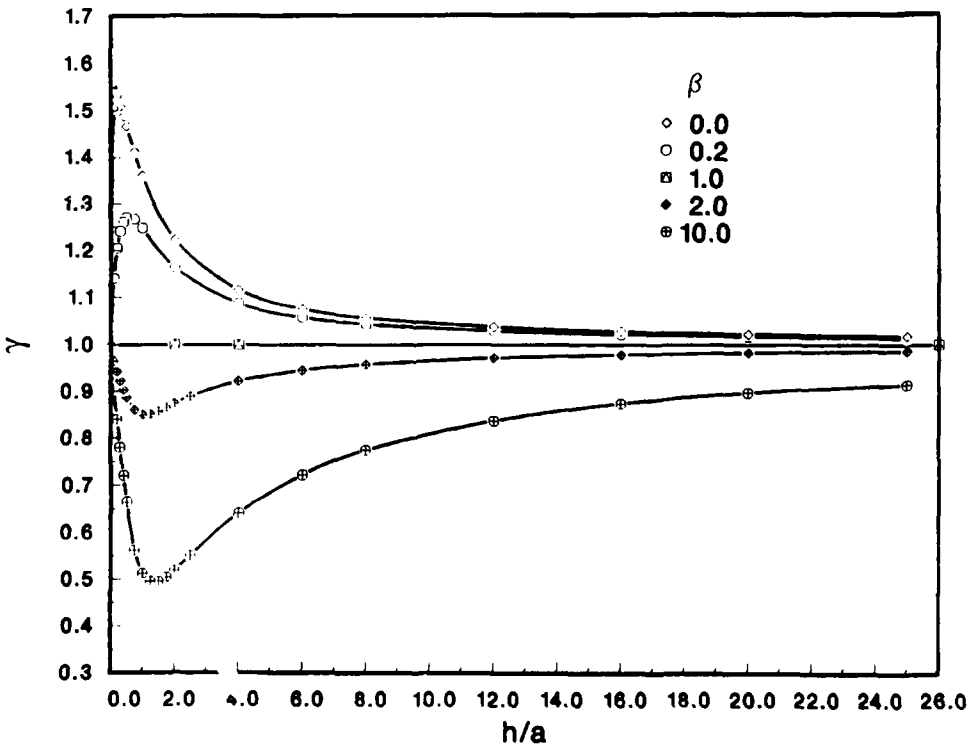

Fig. 6 — Variation of the normalized radius of the contact area between the conical indenter and the perfectly bonded composite medium γ, with layer thickness h/a, as a function of layer/substrate stiffness ratio β ($\nu_1 = \nu_2 = 0.3$)

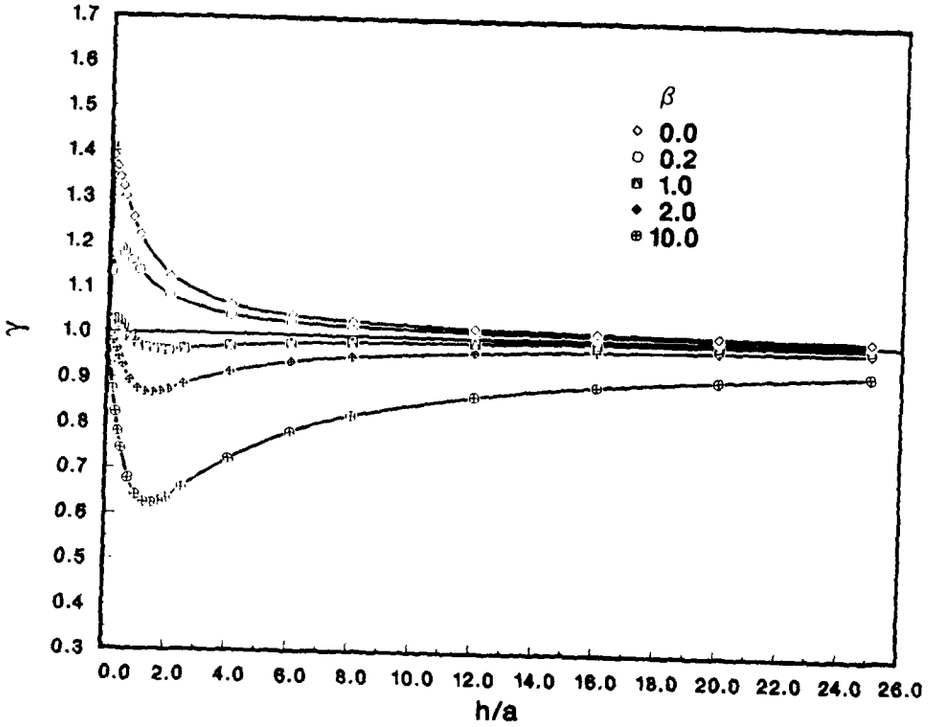

Fig. 7 — Variation of the normalized radius of the contact area between the spherical indenter and the perfectly bonded composite medium γ, with layer thickness h/a as a function of layer/substrate stiffness ratio β ($\nu_1 = \nu_2 = 0.3$)

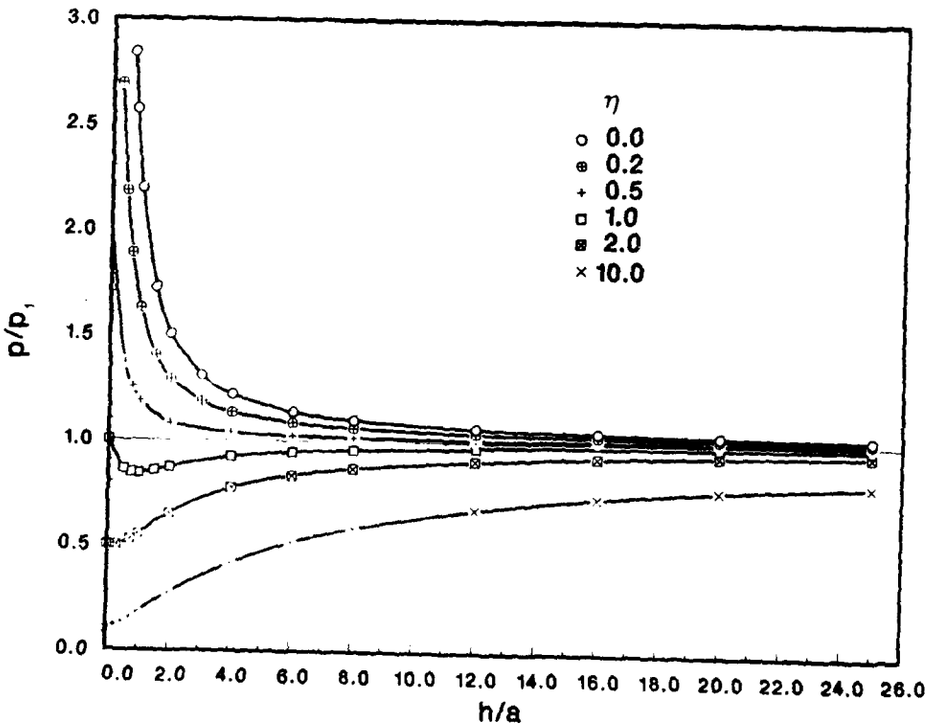

Fig. 8 — Variation of the normalized load p/p_1 for the flat-ended cylindrical indenter with layer thickness h/a for a smooth contact composite medium as a function of layer/substrate stiffness ratio, η

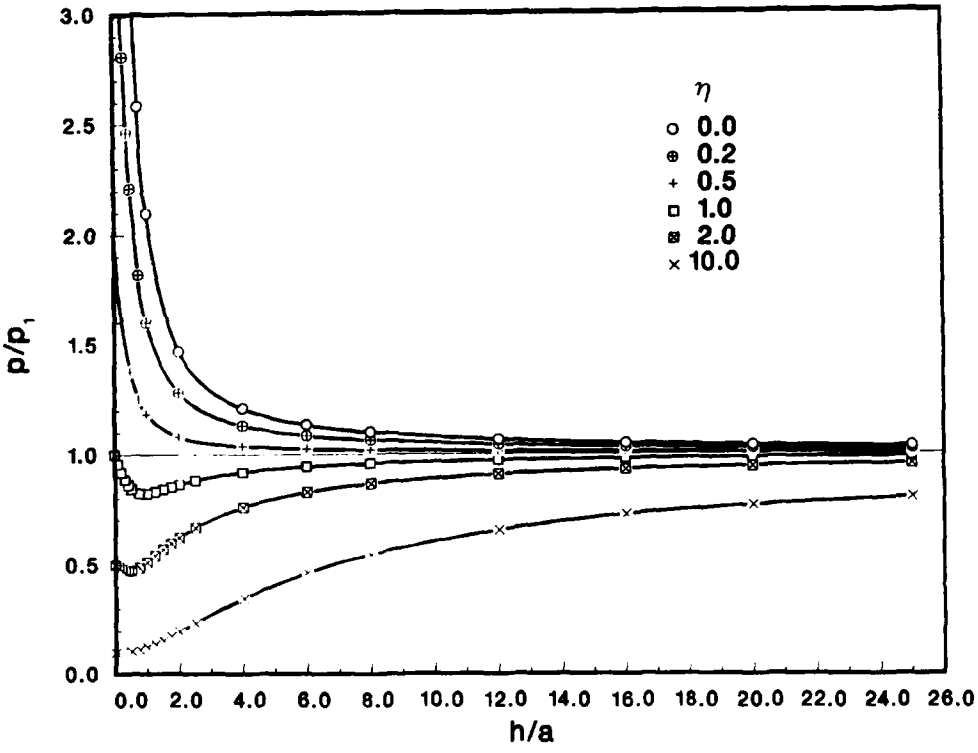

Fig. 9 — Variation of the normalized load p/p_1 for the conical indenter with layer thickness h/a for a smooth contact composite medium as a function of layer/substrate stiffness ratio η

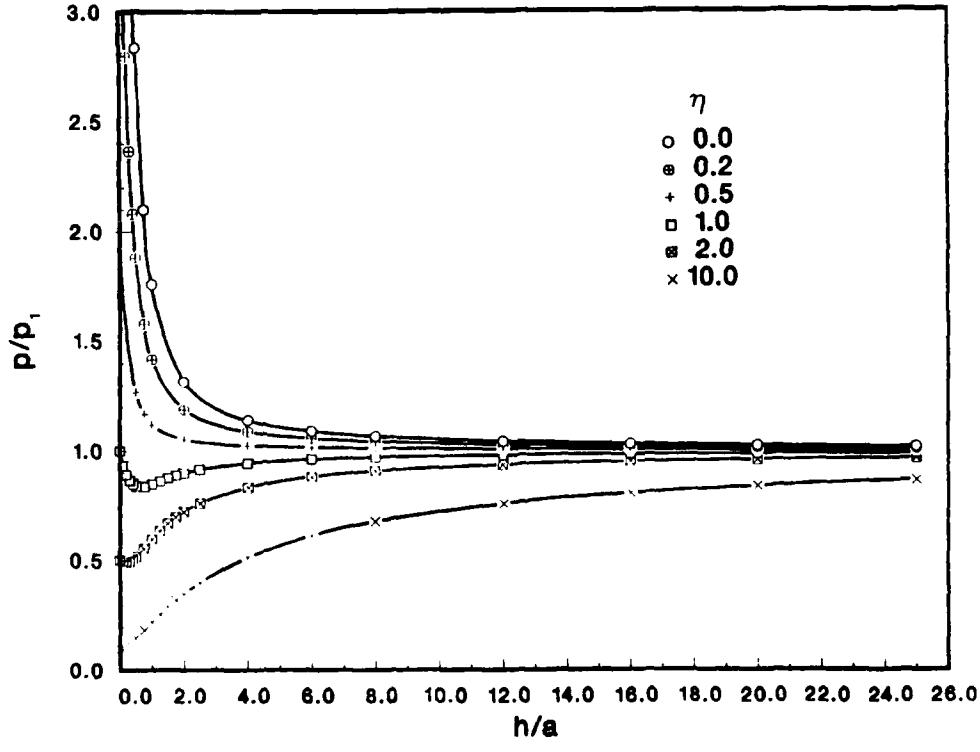

Fig. 10 — Variation of the normalized load p/p_1 for the spherical indenter with layer thickness h/a for a smooth contact composite medium as a function of layer/substrate stiffness ratio η

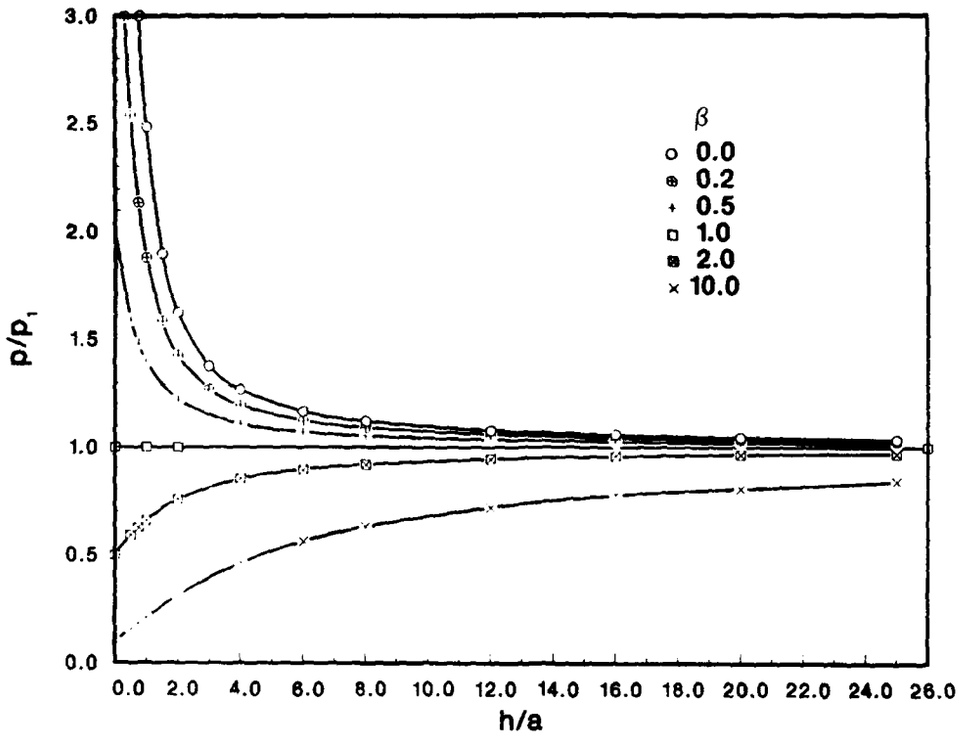

Fig. 11 — Variation of the normalized load p/p_1 for the flat-ended cylindrical indenter with layer thickness h/a for a perfectly bonded composite medium as a function of layer/substrate stiffness ratio β ($\nu_1 = \nu_2 = 0.3$)

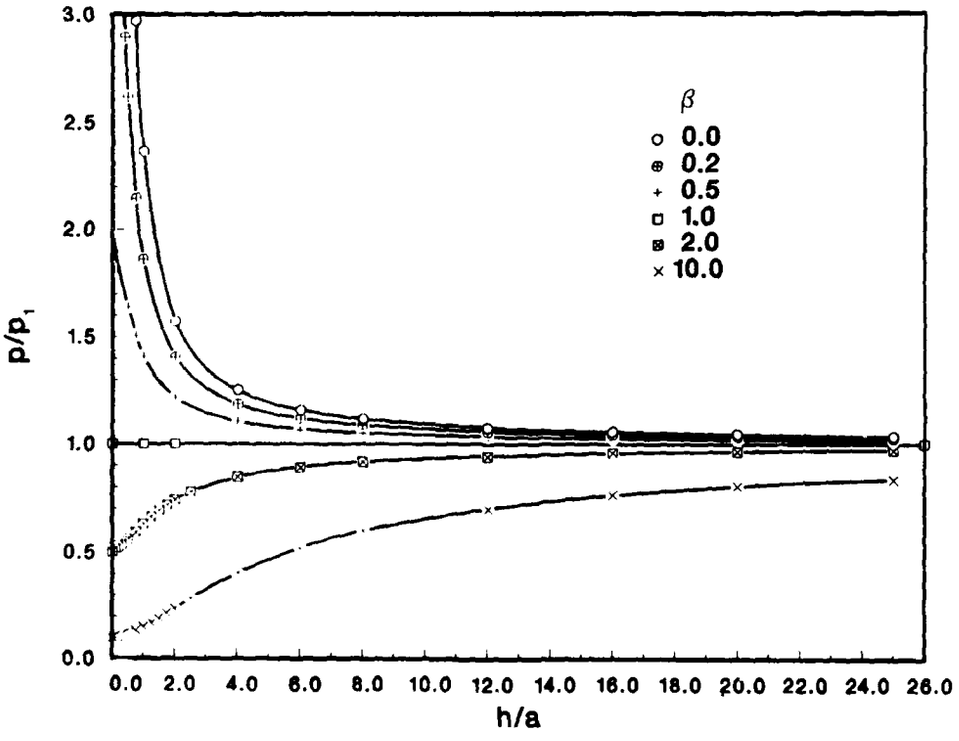

Fig. 12 — Variation of the normalized load p/p_1 for the conical indenter with layer thickness h/a for a perfectly bonded composite medium as a function of layer/substrate stiffness ratio β ($\nu_1 = \nu_2 = 0.3$)

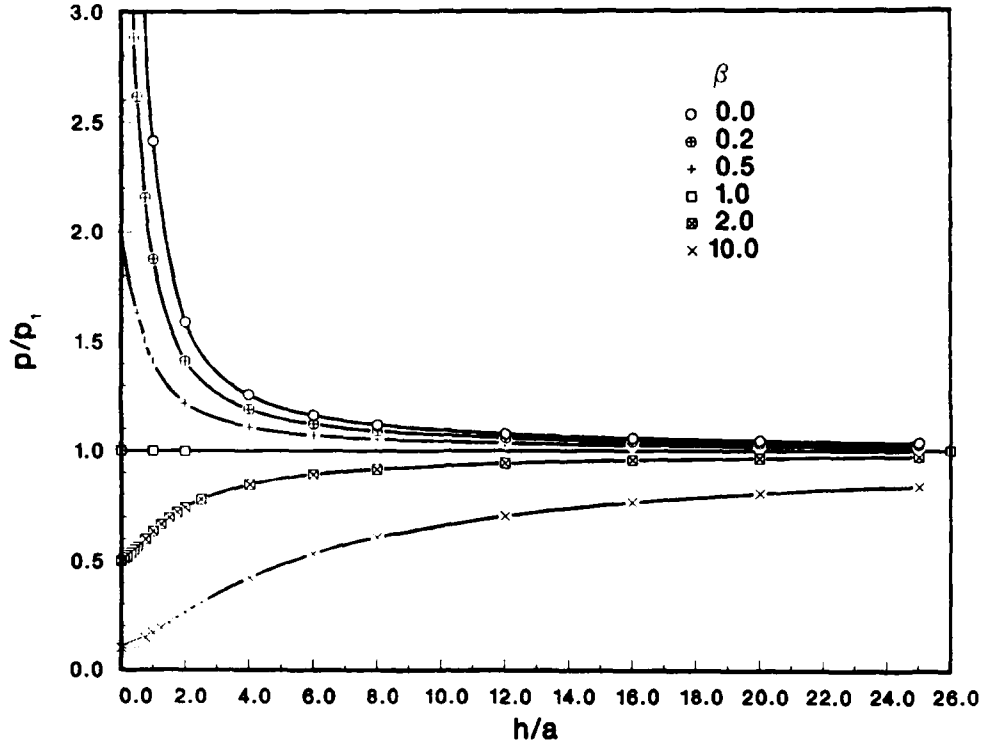

Fig. 13 — Variation of the normalized load p/p_1 for the spherical indenter with layer thickness h/a for a perfectly bonded composite medium as a function of layer/substrate stiffness ratio β ($\nu_1 = \nu_2 = 0.3$)

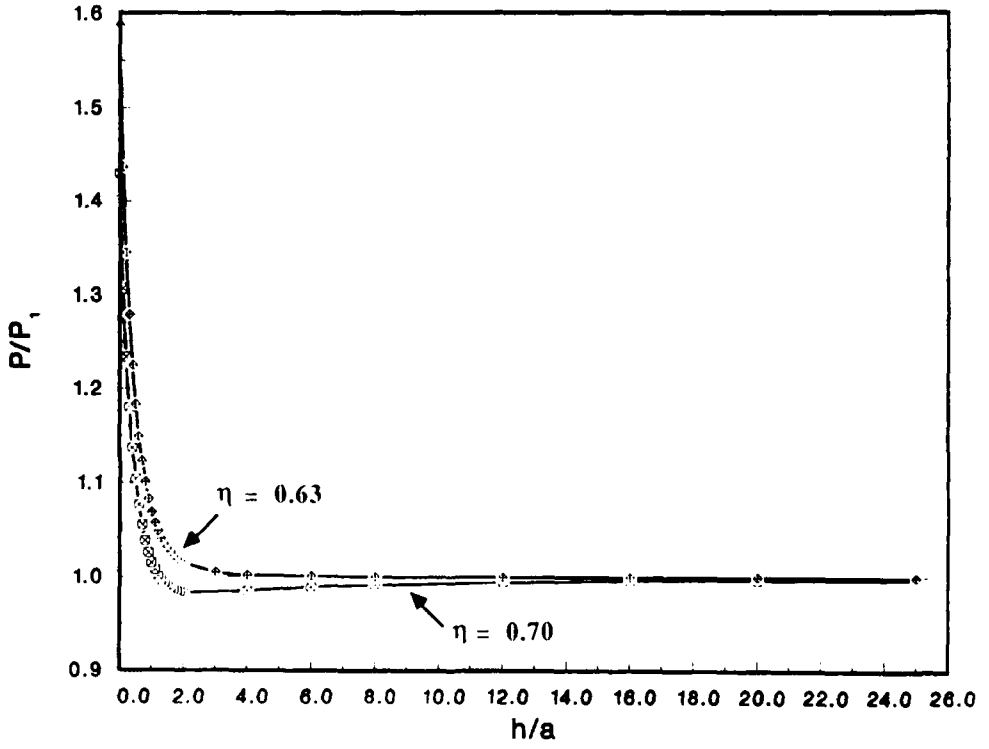

Fig. 14 — Variation of the normalized load p/p_1 for the flat-ended cylindrical indenter with layer thickness h/a for a smooth contact composite medium as a function of layer/substrate stiffness ratio η

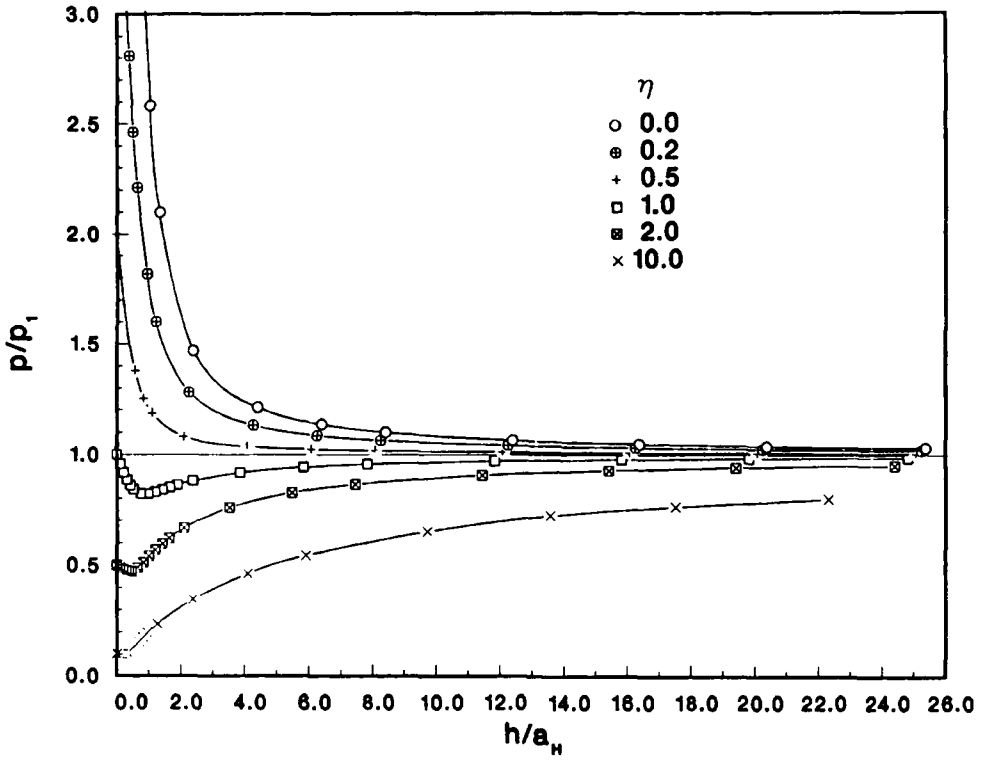

Fig. 15 — Variation of the normalized load p/p_1 for the conical indenter with layer thickness h/a_H for a smooth contact composite medium as a function of layer/substrate stiffness ratio η

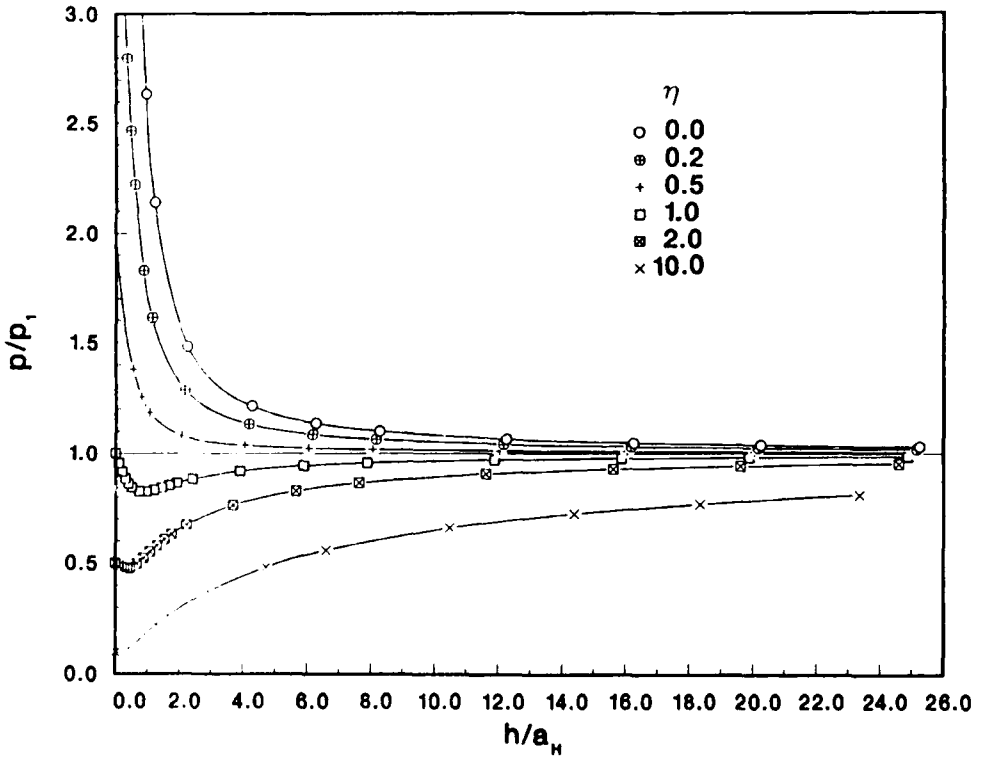

Fig. 16 — Variation of the normalized load p/p_1 for the spherical indenter with layer thickness h/a_H for a smooth contact composite medium as a function of layer/substrate stiffness ratio η

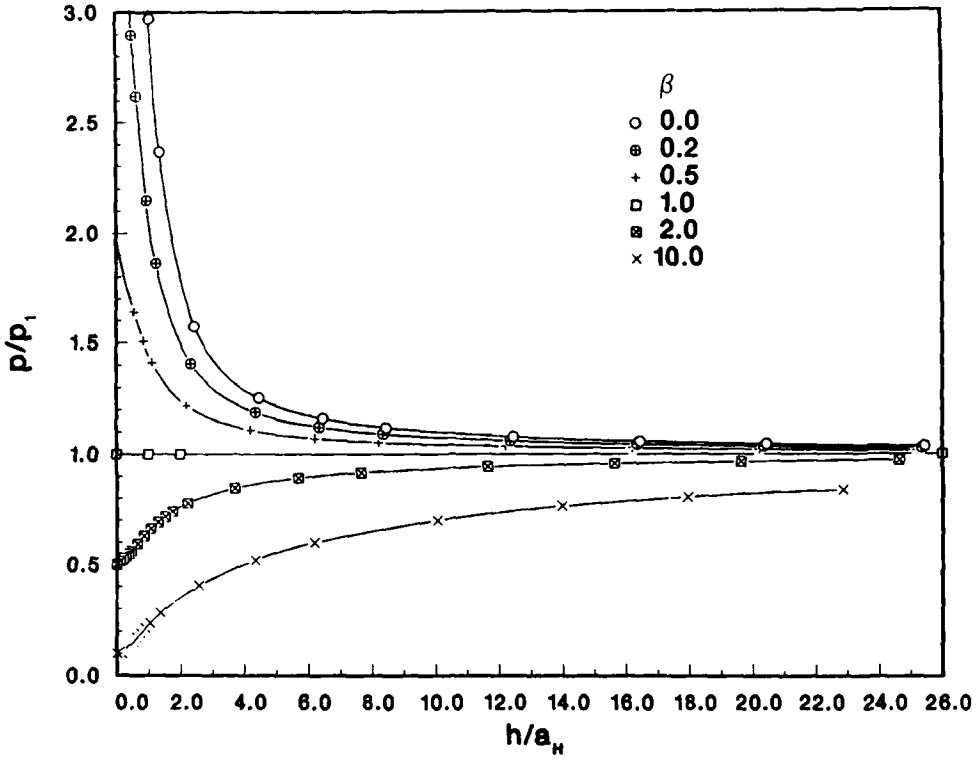

Fig. 17 — Variation of the normalized load p/p_1 for the conical indenter with layer thickness h/a_H for a perfectly bonded composite medium as a function of layer/substrate stiffness ratio β ($\nu_1 = \nu_2 = 0.3$)

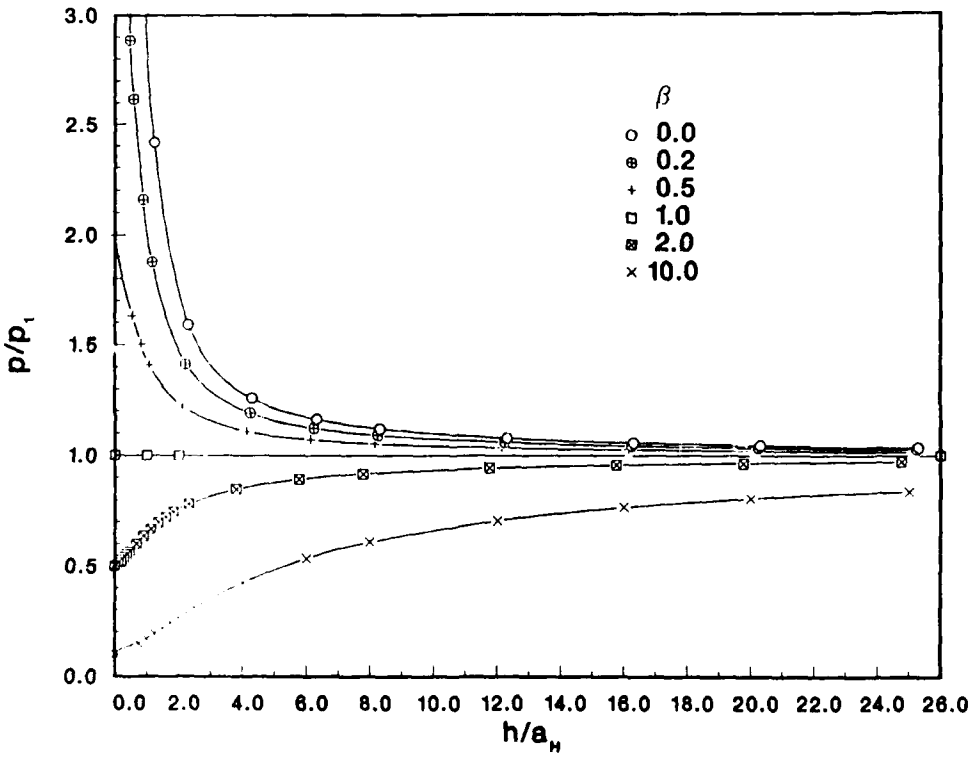

Fig. 18 — Variation of the normalized load p/p_1 for the spherical indenter with layer thickness h/a_H for a perfectly bonded composite medium as a function of layer/stiffness ratio β ($\nu_1 = \nu_2 = 0.3$)

In comparing these results, it is noted that the curves are quite similar for all three types of indenters despite the large differences in values of p and p_1 for the different indenters. This similarity allows us to establish guidelines for choosing a priori the approximate film thickness and substrate elastic properties for determining the elastic constants of the film within a given degree of accuracy. Figures 19 and 20 show, for the perfectly bonded and smooth contact conditions respectively, the film thickness needed so that the absolute values of $(p - p_1)/p_1$ are equal to 2%, 5%, and 10%. Note that the absolute value of the ratio $(p - p_1)/p_1$ has the same value as the ratio of the impression modulus $(\zeta_e - \zeta_1)/\zeta_1$, where ζ_e is the experimentally measured impression modulus obtained according to Eqs. (30), (34), or (41).

To determine the elastic constants of a perfectly bonded layer by the indentation test, as one may expect, the most proper substrate is the one that has the same elastic constants as the layer itself, i.e., $\beta = 1$. Figure 19 shows that when the β value is different from 1, the normalized layer thickness, h/a_H, needed to obtain a given accuracy varies almost linearly with β. The slope of the variation is dependent on the accuracy. The higher the accuracy required the steeper the slope is. When the layer is in smooth contact with the substrate, the best candidate substrate is no longer the one that has the same elastic constants as that of the layer. In this case, the substrate should be slightly stiffer than the layer. By assuming $\nu_1 = \nu_2 = 0.3$, η (in this case equal to β) is found to range from 0.87 (for 10% accuracy) to 0.71 (for 2% accuracy). For values of h/a_H greater than approximately 3, the layer normalized thickness h/a_H needed to obtain a given accuracy also varies almost linearly with η.

In preparing thin films, the film is neither perfectly bonded to the substrate, nor in perfectly smooth contact with the substrate. Figure 21 gives the upper bound h/a_H vs μ_1/μ_2 (by assuming $\nu_1 = \nu_2 = 0.3$) relations to ensure one can measure the film's elastic constants on the composite by the indentation test to a given degree of accuracy. Figure 21 is obtained by taking the upper ranges of the curves from Figs. 19 and 20. This result suggests that a good substrate candidate material is about 25% stiffer than the film material regardless of bonding conditions.

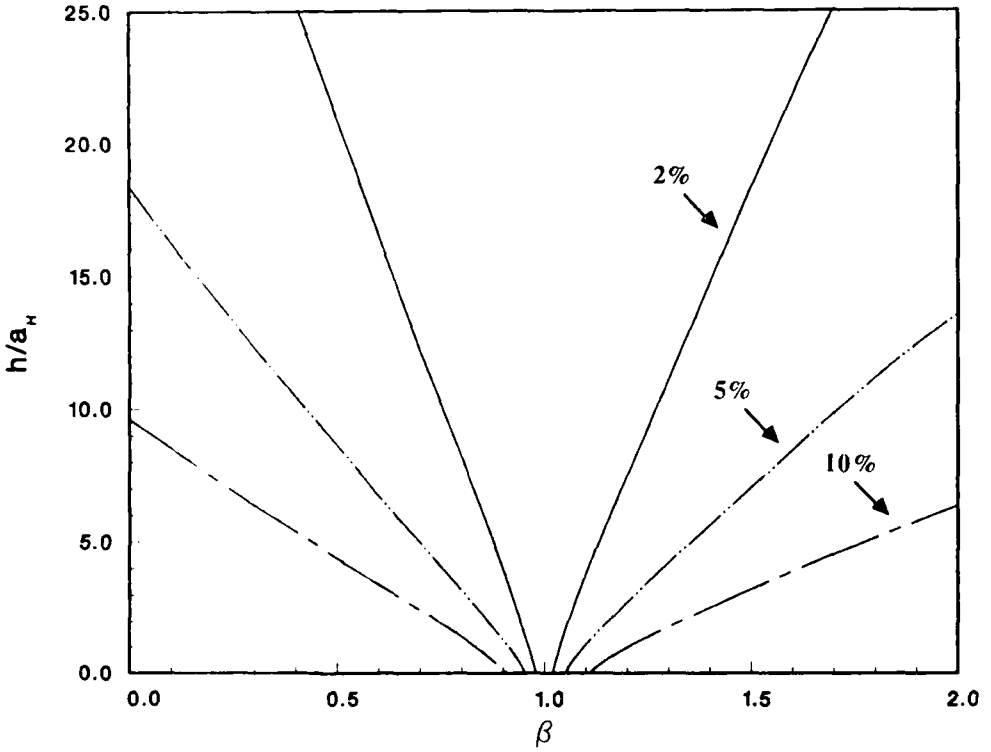

Fig. 19 — Relationships between the layer thickness h/a_H and layer/substrate stiffness ratio β such that $|(p - p_1)/p_i|$ is equal to 2%, 5%, and 10%

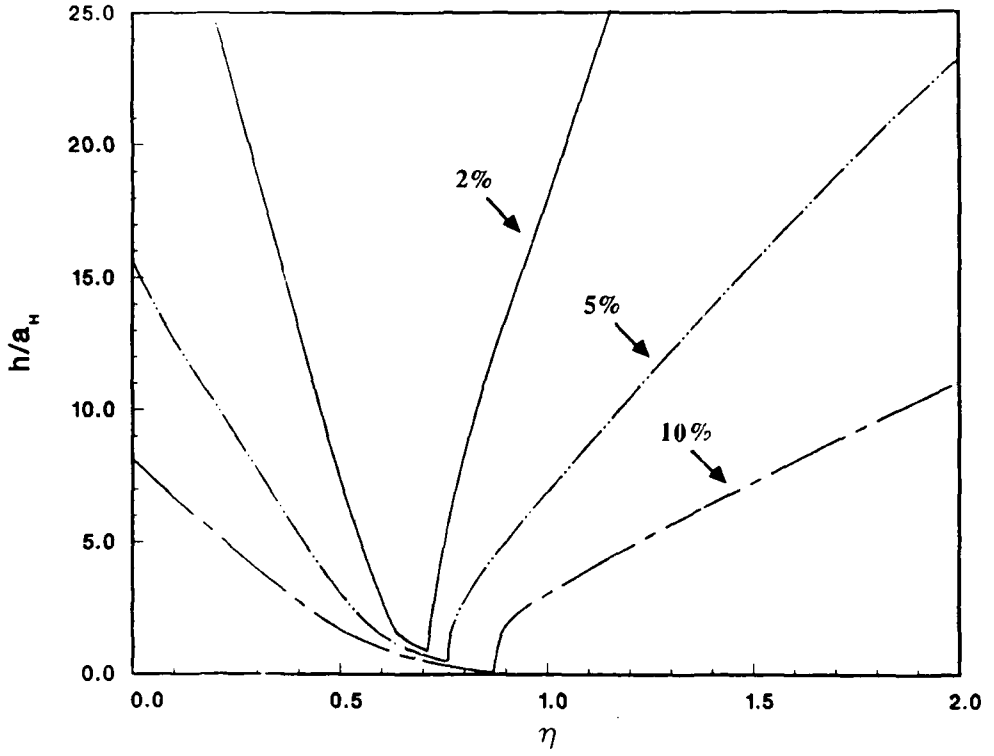

Fig. 20 — Relationships between the layer thickness h/a_H and layer/substrate stiffness ratio η such that $|(p - p_1)/p_1|$ is equal to 2%, 5%, and 10%

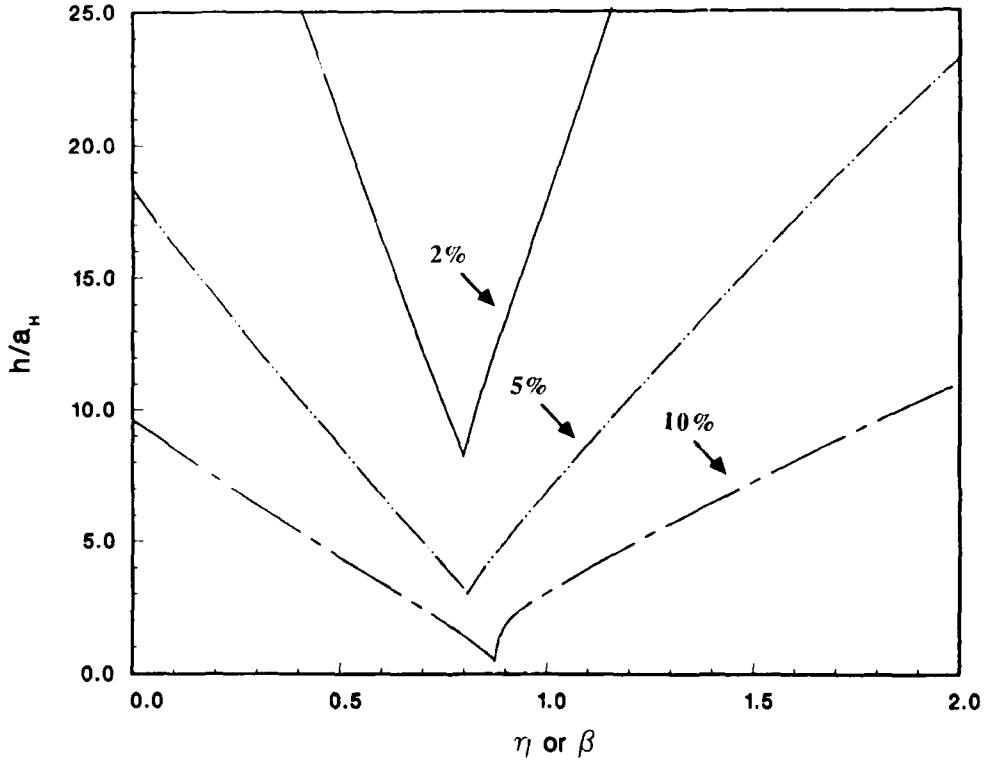

Fig. 21 — Relationships between the layer thickness h/a_H and layer/substrate stiffness ratio η or β such that $|(p - p_1)/p_1|$ is equal to 2%, 5%, and 10%

SUMMARY

The elastic solutions for the stress fields in a composite medium consisting of an elastic layer either perfectly bonded or smoothly overlaying an elastic semi-infinite substrate have been obtained for the cases when the composite medium is indented by rigid spherical, conical, and flat-ended cylindrical indenters. Numerical results were presented, and guidelines were suggested for the proper choice of approximate layer thickness and substrate elastic properties to determine the elastic constants of the layer within certain predetermined accuracy by using the indentation test.

The following comments may be offered in conclusion:

1. For a given minimum film thickness and a given substrate stiffness, the elastic constants of the film may be determined within a calculated accuracy for the cases when the film is perfectly bonded to or in frictionless contact with the substrate. Conversely, if a given accuracy is desired, the required substrate stiffness for a given film thickness or the required minimum film thickness for a given substrate stiffness may be calculated.

2. In presenting the effect of film thickness on indenter load, the film thickness h should be normalized with respect to the Hertz radius a_H of the contact area for the homogeneous half-space instead of normalizing it with respect to the actual radius a of contact area for the composite. The reasons for this are: the value a is not a readily measured quantity because of its dependence on the film thickness and the elastic constants of each component of the composite, whereas a_H can be obtained simply by knowing the penetration depth and the indenter geometry.

3. When $h/a \geq 4$, the load vs film thickness for the composite depends on the film/substrate stiffness ratio and it is not the same as for the homogeneous half-space as suggested elsewhere [12].

4. The p/p_1 vs h/a_H relationships for three different shapes of indenters—conical, spherical, and flat-ended cylindrical—are quite similar despite the large differences in values of p and p_1 for the different indenters.

5. It should be pointed out that this analytical approach is directly applicable to problems in other engineering disciplines such as, for example, the design of large columns on elastic foundations.

REFERENCES

1. R.W. Armstrong and W.H. Robinson, *N.Z. J. Sci.* **17**, 429 (1974).

2. R.W. Armstrong and W.H. Robinson, *J. Mater. Sci.* **10**, 1655 (1975).

3. H.Y. Yu, M.A. Imam, and B.B. Rath, *J. Mater. Sci.* **20**, 636 (1985).

4. M.F. Doerner and W.D. Dix, *J. Mater. Res.* **1**, 601 (1986).

5. J.W. Harding and I.N. Sneddon, *Proc. Cambridge Philos. Soc.* **41**, 16 (1945).

6. I.N. Sneddon, *Int. J. Eng. Sci.* **3**, 47 (1965).

7. R. Muki, *Progress in Solid Mechanics* (North Holland Co., 1960), Vol. 1.

8. N.N. Lebedev and I.S. Ufliand, *PPM* **22**, 320 (1958).

9. T.S. Wu and Y.P. Chiu, *Q. Appl. Math.* **25**, 233 (1967).

10. R. Dhaliwal, *Int. J. Eng. Sci.* **8**, 273 (1970).

11. R. Dhaliwal and I. Rau, *Int. J. Eng. Sci.*, **8**, 483 (1970).

12. W.T. Chen and P.A. Engel, *Int. J. Solids Structures* **8**, 1257 (1972).

13. S.E. El-gendi, *Computer J.* **12**, 282 (1969).

Appendix A

DETERMINATION OF THE FUNCTION $g(\lambda)$

THE PERFECTLY BONDED CASE

When the elastic layer is perfectly bonded to the elastic half-space (substrate), the boundary conditions at the interface $z = h$ are given by Eq. (8). By substituting Eqs. (1) and (2) into Eq. (8), the following simultaneous linear equations of the functions $A_i(\lambda)$, $(i = 1, 2, \ldots, 6)$ can be obtained:

$$w \operatorname{cth} w\, A_1 + w\, A_2 + A_3 + \operatorname{cth} w\, A_4 - \beta w\, A_5 - \beta A_6 = 0,$$

$$(k_1 \operatorname{cth} w - w)A_1 + (k_1 - w \operatorname{cth} w)A_2 - \operatorname{cth} w\, A_3 - A_4$$

$$- \beta(k_2 + w)A_5 - \beta A_6 = 0,$$

$$[2(1 - \nu_1) - w \operatorname{cth} w]\, A_1 + [2(1 - \nu_1) \operatorname{cth} w - w]A_2 - A_3 - \operatorname{cth} w\, A_4 \qquad \text{(A1)}$$

$$+ [2(1 - \nu_2) + w]\, A_5 + A_6 = 0,$$

$$[w - (1 - 2\nu_1) \operatorname{cth} w]\, A_1 + [w \operatorname{cth} w - (1 - 2\nu_1)]\, A_2 + \operatorname{cth} w\, A_3 + A_4$$

$$+ [(1 - 2\nu_2) + w]\, A_5 + A_6 = 0,$$

where $\beta = \mu_1/\mu_2$ and $w = \lambda h$. By solving Eqs. (4.3), (5), and (A1), the function $g(\lambda)$ for the perfectly bonded condition can be expressed as:

$$g(\lambda) = 1 - \frac{(B_1 + B_2 w + B_3 \operatorname{sh}^2 w)\, e^{-w} + (B_4 + B_5 w + B_6 \operatorname{sh}^2 w) \operatorname{sh} w}{(C_1 + C_2 w^2 + C_3 \operatorname{sh}^2 w) e^{-w} + (C_4 + C_5 w^2 + B_6 \operatorname{sh}^2 w) \operatorname{sh} w}, \qquad \text{(A2)}$$

where

$$B_1 = 4a_1 a_2 (1 + b_2 \beta)\beta,$$

$$B_2 = -1 - 3b_2\beta + (k_2 - 2b_2^2)\beta^2 + b_2 k_2 \beta^3,$$

$$B_3 = 2a_2(1 + 2k_1 + 2b_2 k_1 \beta + k_2 \beta^2)\beta,$$

$$B_4 = k_1 + (-b_2 + 2b_2 k_1 + 4a_1 a_2)\beta + (k_1 + 4a_1 a_2 k_2 + 2b_1 b_2^2)\beta^2 + b_2 k_2 \beta^3,$$

$$
\begin{aligned}
B_5 &= -1-(1+4b_2)\,\beta + (1-2b_2)k_2\beta^2 + k_2^2\beta^3,\\
B_6 &= k_1 + (1+2k_1k_2)\,\beta + (k_2 + 4a_2b_2k_1 + 16a_1a_2^2 + 2b_1b_2^2)\,\beta^2 + k_2^2\beta^3,\\
C_1 &= 4a_1^2\,(1+b_2\beta),\\
C_2 &= 1 + 3b_2\beta - (k_2 - 2b_2^2)\,\beta^2 - b_2k_2\beta^3,\\
C_3 &= k_1 - (1-2k_1)b_2\beta + (k_2 + 16a_1a_2^2 + 2b_1b_2^2)\,\beta^2 + b_2k_2\beta^3,\\
C_4 &= 4a_1^2 + 4a_1(2a_2 + a_1k_2)\,\beta - 8a_1a_2b_2\beta^2,\\
C_5 &= 1 + (k_2 + 2b_2)\beta - (1-2b_2)k_2\beta^2 - k_2^2\beta^3,
\end{aligned}
\tag{A3}
$$

and

$$a_1 = 1-\nu_1,\ a_2 = 1-\nu_2,\ b_1 = 1-2\nu_1,\ b_2 = 1-2\nu_2,\ k_1 = 3-4\nu_1,\ \text{and}\ k_2 = 3-4\nu_2.$$

For the homogeneous half-space consisting of layer material, i.e., $h \to \infty$, Eq. (A2) gives $g(\lambda) = 0$. Then by Eq. (20) we have $k(u) = 0$ and Eq. (6) becomes

$$
\begin{aligned}
&\int_0^\infty M(\lambda)J_0(\lambda r)\,d\lambda = f(r) \qquad (0 \le r \le a),\\
&\int_0^\infty \lambda M(\lambda)J_0(\lambda r)\,d\lambda = 0 \qquad (a < r < \infty),
\end{aligned}
\tag{A4}
$$

and Eqs. (17) and (19) give an explicit expression for the function $H(\tau)$, namely

$$H(\tau) = F_0(\tau) = 1 - \frac{\delta(0)}{d} - \frac{\tau}{d}\int_0^{\frac{\pi}{2}} \delta'(\tau \sin\theta)d\theta. \tag{A5}$$

This result is the same as those obtained by many authors [A1] for the homogeneous half-space. On the other hand, when $h \to 0$, i.e., a homogeneous half-space with elastic constants μ_2 and ν_2, Eq. (A2) gives

$$g(\lambda) = 1 - \eta, \tag{A6}$$

where

$$\eta = \frac{(1-\nu_2)\mu_1}{(1-\nu_1)\mu_2}. \tag{A7}$$

Substituting Eq. (A6) into Eq. (6) gives

$$\int_0^\infty M^*(\lambda)J_0(\lambda r)\,d\lambda = f(r)/\eta \qquad (0 \le r \le a),$$

and

$$\int_0^\infty \lambda M^*(\lambda) J_0(\lambda r)\, d\lambda = 0 \qquad (a < r < \infty), \tag{A8}$$

where

$$M^*(\lambda) = M(\lambda)/\eta.$$

By using Eq. (A7) for η and Eq. (7) for $f(r)$, Eq. (A8) assumes the same form as Eq. (A4) for the homogeneous half-space with elastic constants μ_2 and ν_2.

THE SMOOTH CONTACT CASE

When the elastic layer is in smooth (frictionless) contact with the surface of the elastic substrate, the simultaneous linear equations of the functions $A_i(\lambda)$, $(i = 1, 2, \ldots, 6)$ can be obtained by substituting Eqs. (1) and (2) into Eq. (9), thus

$$\begin{aligned}
&(k_1 \operatorname{cth} w - w) A_1 + (k_1 - w \operatorname{cth} w) A_2 - \operatorname{cth} w\, A_3 - A_4 - \beta(k_2 + w) A_5 - \beta A_6 = 0,\\
&[2(1 - \nu_1) - w \operatorname{cth} w] A_1 + [2(1 - \nu_1) \operatorname{cth} w - w] A_2 - A_3 - \operatorname{cth} w\, A_4\\
&\qquad + [2(1 - \nu_2) + w] A_5 + A_6 = 0,\\
&[w - (1 - 2\nu_1) \operatorname{cth} w] A_1 + [w \operatorname{cth} w - (1 - 2\nu_1)] A_2 + \operatorname{cth} w\, A_3 + A_4 = 0,\\
&[(1 - 2\nu_2) + w] A_5 + A_6 = 0.
\end{aligned} \tag{A9}$$

Equations (4.3) and (A9) give

$$g(\lambda) = 1 - \frac{\operatorname{sh}^2 w + \eta\,(w + \operatorname{sh} w \operatorname{ch} w)}{w + \operatorname{sh} w \operatorname{ch} w + \eta\,(\operatorname{sh}^2 w - w^2)}. \tag{A10}$$

For the homogeneous half-space, Eq. (A10) gives

$$g(\lambda) = 0 \qquad h \to \infty$$

and

$$g(\lambda) = 1 - \eta \qquad h \to 0,$$

which are the same as for the case when the layer is perfectly bonded to the substrate.

REFERENCES

A1. T.S. Wu and Y.P. Chin, *Q. Appl. Math.* **25**, 233 (1967).

Appendix B

COMPARISON OF NUMERICAL RESULTS

The following tables list some of the numerical results obtained by the authors and those given by other authors [B1-B3]. Tables B1 and B2 show the numerical values of the kernel $K(u)$ and function $H(\tau)$, respectively, for a flat-ended cylindrical indenter on a layer that is in smooth contact to a rigid substrate. In these two tables, the data on the second and the fourth columns are obtained by the present analysis and data on the first and the third columns are those listed on the first and the fourth columns of Tables I and II of Lebedev and Ufliand paper [B1]. The agreement among these data shows that we can reproduce their results in this special case.

Table B3 shows our values and those of Dhaliwal's [B2] (the first and the last columns on Table 2 for $\beta = 0$ and 0.25 in Ref. B2) for the Kernel $K(u)$ for a flat-ended cylindrical indenter on a layer that is perfectly bonded to an elastic half-space. The good agreement between these results provided a check of our formulation of the function $g(w)$ for the perfectly bonded condition, which is rather complicated to check otherwise. However, by using the same set of values of the kernel $K(u)$ shown in Table B3, we cannot reproduce Dhaliwal's results for the $H(\tau)$ values. These two sets of data are compared in Table B4. In some cases (e.g., $h/a = 0.25$), there are order of magnitude differences. Chen and Engel [B3] have pointed out that they could not reproduce all of Dhaliwal's results.

Table B1 — Numerical Value of the Kernel $K(u)$ for a Flat-Ended Cylindrical Indenter on a Film in Smooth Contact with a Rigid Half-Space.

u	$h/a = 2.0$		$h/a = 0.5$	
	LU[a]	YSR[b]	LU	YSR
0.0	0.5837	0.58379	2.3349	2.33515
0.2	0.5798	0.57985	2.0990	2.09873
0.4	0.5682	0.56824	1.5513	1.55130
0.6	0.5496	0.54955	0.9875	0.98751
0.8	0.5248	0.52468	0.5753	0.57516
1.0	0.4948	0.49479	0.3279	0.32805
1.2	0.4612	0.46114	0.1962	0.19621
1.4	0.4251	0.42507	0.1291	0.12908
1.6	0.3878	0.38783	0.0939	0.09396
1.8	0.3505	0.35053	0.0737	0.07367
2.0	0.3141	0.31414	0.0602	0.06029

[a] Results from Lebedev and Ufliand [B1].
[b] Results from present report.

Table B2 — Numerical Value of the Function $H(\tau)$ for a Flat-Ended Cylindrical Indenter on a Film in Smooth Contact with a Rigid Half-Space

τ	$h/a = 2.0$		$h/a = 0.5$	
	LU[a]	YSR[b]	LU	YSR
0.0	1.530	1.5305	4.321	4.3303
0.1	1.529	1.5297	4.303	4.3111
0.2	1.527	1.5274	4.246	4.2584
0.3	1.523	1.5236	4.153	4.1680
0.4	1.518	1.5183	4.022	4.0382
0.5	1.511	1.5116	3.854	3.8693
0.6	1.503	1.5036	3.650	3.6642
0.7	1.494	1.4943	3.416	3.4277
0.8	1.484	1.4839	3.157	3.1671
0.9	1.472	1.4723	2.884	2.8919
1.0	1.460	1.4598	2.608	2.6138

[a] Results from Lebedev and Ufliand [B1].
[b] Results from present report.

Table B3 — Numerical Value of the Kernel $K(u)$ for a Flat-Ended Cylindrical Indenter on a Film Perfectly Bonded to an Elastic Half-Space

$\nu_1 = 0.333$, $\nu_2 = 0.250$					
β	u	$h/a = 3.0$		$h/a = 0.25$	
		Dha[a]	YSR[b]	Dha	YSR
0.00	0.0	−0.150197	−0.150197	−1.802363	−1.80236
	0.2	−0.149575	−0.149575	−1.028806	−1.02881
	0.4	−0.147729	−0.147729	−0.278302	−0.278302
	0.6	−0.144714	−0.144714	−0.085151	−0.085151
	0.8	−0.140617	−0.140617	−0.044783	−0.044783
	1.0	−0.135556	−0.135556	−0.028933	−0.028933
	1.2	−0.129669	−0.129670	−0.020056	−0.020056
	1.4	−0.123110	−0.123110	−0.014720	−0.014720
	1.6	−0.116038	−0.116038	−0.011301	−0.011301
	1.8	−0.108616	−0.108616	−0.008969	−0.008969
	2.0	−0.100997	−0.100997	−0.007297	−0.007298
0.25	0.0	−0.106266	−0.106559	−1.275187	−1.27871
	0.2	−0.105844	−0.106137	−0.746888	−0.749318
	0.4	−0.104594	−0.104885	−0.213979	−0.214720
	0.6	−0.102551	−0.102838	−0.062722	−0.062538
	0.8	−0.099773	−0.100055	−0.029314	−0.028821
	1.0	−0.096338	−0.096613	−0.018148	−0.017619
	1.2	−0.092337	−0.092604	−0.012580	−0.012105
	1.4	−0.087871	−0.088129	−0.009338	−0.008939
	1.6	−0.083047	−0.083296	−0.007270	−0.006942
	1.8	−0.077073	−0.078211	−0.005849	−0.005581
	2.0	−0.072751	−0.072978	−0.004818	−0.004597

[a] Results from Dhaliwal [B2].
[b] Results from present report.

Table B4 — Numerical Value of the Function $H(\tau)$ for a Flat-Ended Cylindrical Indenter on a Film Perfectly Bonded to a Elastic Half-Space.

$\nu_1 = 0.333$, $\nu_2 = 0.250$					
β	τ	$h/a = 3.0$		$h/a = 0.25$	
		Dha[a]	YSR[b]	Dha	YSR
0.00	0.0	1.461578	1.40430	119.6635	10.7832
	0.1	1.461143	1.40392	114.7609	10.7302
	0.2	1.459840	1.40277	103.0672	10.5697
	0.3	1.457678	1.40087	89.7998	10.2972
	0.4	1.454671	1.39823	77.4355	9.90395
	0.5	1.450839	1.39486	67.27787	9.37582
	0.6	1.446208	1.39079	57.93688	8.69071
	0.7	1.440806	1.38604	49.18944	7.81816
	0.8	1.434670	1.38065	40.61215	6.73197
	0.9	1.427838	1.37464	31.97879	5.45602
	1.0	1.420351	1.36806	23.50496	4.12980
0.25	0.0	1.289450	1.25805	4.120174	3.03548
	0.1	1.289188	1.25781	4.025767	3.03001
	0.2	1.288405	1.25711	3.806495	3.01305
	0.3	1.287105	1.25595	3.570212	2.98279
	0.4	1.285298	1.25434	3.368143	2.93574
	0.5	1.282993	1.25228	3.197656	2.86600
	0.6	1.280207	1.24978	3.036678	2.76393
	0.7	1.276957	1.24688	2.860609	2.61524
	0.8	1.273263	1.24358	2.644312	2.40384
	0.9	1.269148	1.23990	2.368507	2.12545
	1.0	1.264636	1.23586	2.039119	1.80981

[a] Results from Dhaliwal [B2].
[b] Results from present report.

Table B5 gives both Chen and Engel's results (Table II in Ref. B3) and our results for the values p^* and d^* for a spherical indenter ($a << R$) on a layer that is in smooth contact with an elastic half-space ($b = 0.1$, $\nu_1 = \nu_2 = 0.3$). The agreement between these two sets of results in excellent only at large h/a values. The reason for the discrepancy at low h/a values is believed to be due to the approximation method used by Chen and Engel. In their analysis, they introduce a "perturbing term" in the expression of the contact pressure. Our comment is that when the elastic properties of the substrate are quite different from that of the layer, or the layer becomes thin enough, then the difference between the contact pressure for the composite and those for the corresponding homogeneous half-space is large enough such that the perturbation approach is no longer appropriate.

It seems to us that the nondimensional quantities p^* and δ^* defined by Chen and Engel [B3] are quite ambiguous. According to their definitions, the p^* and the δ^* can be written as

$$p^* = \frac{p}{p_1} \frac{1}{\gamma_s^3} \tag{B1}$$

Table B-5 — Numerical Value of the Parameter p^* and δ^* for a Spherical Indenter on a Film in Smooth Contact with and Elastic Half-Space

$\beta = 10.0$, $\nu_1 = \nu_2 = 1/3$				
h/a	p^*		δ^*	
	CE[a]	YSR[b]	CE	YSR
∞	1.0000	1.0000	1.0000	1.0000
16.0	1.0001	1.0001	0.9669	0.9669
8.0	1.0009	1.0009	0.9345	0.9345
4.0	1.0070	1.0070	0.8746	0.8746
2.0	1.0469	1.0469	0.7815	0.7815
1.5	1.0954	1.0954	0.7389	0.7389
1.0	1.2310	1.2309	0.6868	0.6868
0.6	1.5675	1.5680	0.6479	0.6479
0.4	1.9975	1.9971	0.6406	0.6405
0.3	2.3968	2.3960	0.6466	0.6563
0.2	3.0804	3.0846	0.6672	0.6677
0.15	3.6341	3.6485	0.6880	0.6897
0.1	4.4894	4.5130	0.7246	0.7232
0.0	10.0000	10.0000	1.0000	1.0000

[a] Results from Chen and Engel [B3].
[b] Results from present report.
$p^* = p/(p_1\gamma_s^3)$
$\delta^* = a/\gamma_s^2$

and

$$\delta^* = \frac{a}{\gamma_s^2}. \tag{B2}$$

In these expressions, it is clearly seen that p^* is not the load on the indenter for the composite normalized with respect to the corresponding load for the homogeneous half-space, neither it is equal to a_H/a as they claim. The δ^* value presented is not appropriate either because they set a equal to one, which is not correct since, as mentioned previously, the radius of the contact area is not a constant but is a function of the shape of the indenter, the penetration depth, the layer thickness, and the elastic constants of both the layer and the substrate.

REFERENCES

B1. N.N. Lebedev and I.S. Ufliand, *PPM* **22**, 320 (1958).

B2. R. Dhaliwal, *Int. J. Eng. Sci.* **8**, 273 (1970).

B3. W.T. Chen and P.A. Engel. *Int. J. Solids Structures* **8**, 1257 (1972).